Evaluation of a Communication-less and Load-independent Resonance Mismatch Compensation Method for Wireless Power Transfer at Close Coil-to-Coil Distances Using LCC-S Circuits

Yuki Ouchi [1)] Takehiro Imura [1)] Yoichi Hori [1)]

1) Faculty of Science and Engineering, Tokyo University of Science, Noda, Chiba, Japan

E-mail: ouchi.yuki21@gmail.com

ABSTRACT: Wireless power transfer (WPT) for electric vehicles (EV) uses compensation capacitors to adjust the resonant frequency. However, due to the influence of ferrites and aluminum plates, the resonance is shifted when the distance between the coils changes. Resonance mismatch is a cause of deteriorated transmission characteristics. This paper proposes a resonance mismatch compensation method for LCC-S circuit, focusing on the output voltage and independent of load variations. The proposed method does not require any control on the transmitter (Tx) side, and the resonance mismatch compensation is carried out using information only on the receiver (Rx) side, without using communication. To validate the theory, transmission characteristics were evaluated by numerical analysis and experiments. Comparison of the results shows that load-independent resonance mismatch compensation is possible by focusing on the output voltage.

KEY WORDS: Wireless Power Transfer (WPT), Resonance Mismatch, Detuning, Gyrator, LCC Circuit

1. INTRODUCTION

Wireless power transfer (WPT) via magnetic resonance is attracting attention as an effective way of supplying power to electric vehicles (EV) [(1)]. Installing a WPT system on parked EV in parking lots and garages can eliminate the need for manual charging[(2), (3)].

This technology uses compensation capacitors on the transmitter (Tx) and receiver (Rx) sides, respectively, to improve transmission characteristics by adjusting the resonance frequency. [(4)-(6)]. However, the self-inductance of the Tx and Rx coils changes during power transmission in situations where the distance between the Tx-Rx coils is close, such as in SAE J2954 VA Z-classes Z1 [(7)], due to the influence of conductors such as ferrite and aluminum plates often used in the Tx and Rx coils [(8)]. Changes in the self-inductance of the Tx and Rx coils cause resonance mismatch on the Tx and Rx sides, resulting in deterioration of transmission characteristics such as transmitted power and reduced efficiency [(9)-(12)].

Several methods of compensating for resonance mismatch have been proposed in references[(13)-(15)]. Li *et al.*[(13)] proposed a method using communication between Tx and Rx to correct resonance misalignment on the Rx side and then on the Tx side. However, the use of communication is undesirable, for example from the perspective of system complexity. Some methods for compensating for resonance mismatch without the use of communication between Tx and Rx sides have been proposed in references[(14),(15)]. Matsumoto and Fujimoto[(14)] proposed a system that controls the current flowing from the power supply to keep it constant, thus eliminating the need for communication and resonance mismatch compensation on the Tx side and compensating for capacitors on the Rx side. However, the Tx side should be less controlled from the point of view of infrastructure facilities and the cost of burying the Tx side in the road. Matsuura *et al.*[(15)] proposed a system that eliminates the need for control on the Tx side by using LCC circuits and enables communication-less, resonance mismatch compensation based on information from the Rx side only. However, references [(13)-(15)] require the load to be fixed when compensating resonance mismatch, which means that power control, in particular the protection of excess power, cannot be carried out concurrently.

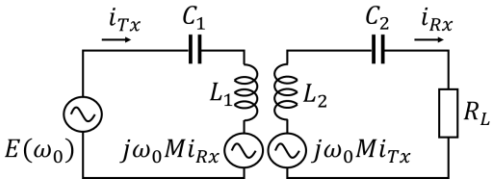

Fig. 1 Equivalent Circuit of S-S Circuit

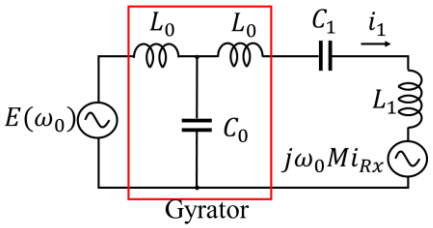

Fig. 2 Gyrator + S Circuit in Tx-side

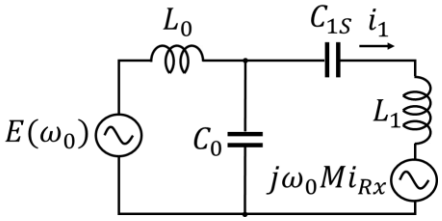

Fig. 3 LCC Circuit

This paper presents a color map of the relationship between resonance mismatch, power and voltage and proposes a compensation method independent of the resistance of the load. The proposed method uses an LCC circuit which adds a compensating inductor and capacitor on the Tx side to eliminate the need for control on the Tx side and correct the resonance mismatch without communication using information only on the Rx side. The theory is verified by manually varying the capacitance and load resistance on the Rx side and evaluating the transmission characteristics through numerical analysis and experimental measurements.

2. A power robustness method against resonance mismatch on the Tx side

In this chapter, robustness against resonance mismatch on the Tx side is described. Fig. 1 shows the equivalent circuit of the S-S circuit widely used in wireless power transfer. For simplicity of analysis, the internal resistance of the Tx and Rx coils is neglected. the induced electromotive force (induced EMF) on the Rx side is proportional to the current i_{Tx} flowing in the Tx coil. Using the current i_{Tx} flowing in the Tx coil, the mutual inductance M, the inductance L_2 of the Rx coil, the capacitance C_2 of the capacitor on the Rx side and the resistance R_L of the load, the power P_{out} consumed by the load can be expressed as follows:

$$P_{out} = \frac{(\omega_0 M i_{Tx})^2 R_L}{R_L^2 + \left(\omega_0 L_2 - \frac{1}{\omega_0 C_2}\right)^2} \quad (1)$$

This means that even when the resonance on the Tx side is shifted, P_{out} remains unchanged if i_{Tx} is constant. In other words, the power can be made robust against resonance mismatch on the Tx side by keeping i_{Tx} constant, irrespective of resonance mismatch on the Tx side. To keep i_{Tx} constant, a constant voltage source is converted into a current source independent of M and the resonance shift by using gyrator characteristics before the S circuit on the Tx side, as shown in Fig. 2. i_1 in Fig. 2 can be expressed as follows:

$$i_1 = \frac{1}{\omega_0 L_0} E \quad (2)$$

This means that i_1 remains constant even when the parameters to the right of the gyrator circuit, such as M, L_1 and C_1, change.

L_0 which is on the right side of the gyrator circuit in Fig. 2 and C_1 in Fig. 2 can also be combined into one as C_{1S}. Fig. 3 shows a circuit combined into one as C_{1S}. This is called an LCC circuit and is widely used in WPT system [16]. From the above, the LCC circuit can be used to stabilize the power without using control against resonance mismatch on the Tx side.

3. Proposed resonance mismatch compensation method in LCC-S circuits

This chapter describes a method for correcting resonance mismatch independent of the load on the Rx side of the proposed method, which combines an LCC circuit on the Tx side and an S circuit with a capacitor added in series with the coil on the Rx side.

3.1. resonance condition

Fig. 4 shows the LCC-S circuit. L_0 represents the compensating inductor of the circuit, C_0, C_{1S}, C_2 the compensating capacitors, L_1, L_2 the self-inductance of the Tx and Rx coils respectively, R_L represents the connected load.

At resonance, the following resonance condition (3) holds for the frequency ω_0 of the power supply and each element in LCC-S circuit.

$$\omega_0 = \frac{1}{\sqrt{L_0 C_0}} = \sqrt{\frac{C_0 + C_{1S}}{L_1 C_0 C_{1S}}} = \frac{1}{\sqrt{L_2 C_2}} \quad (3)$$

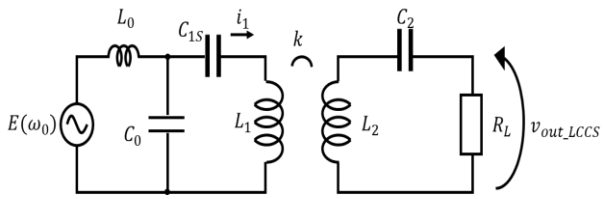

Fig. 4 LCC-S Circuit

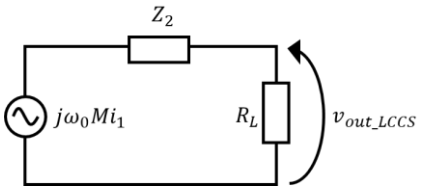

Fig. 5 Equivalent Circuit of Rx side

As described in the previous chapter, the use of LCC on the Tx side eliminates the effect of resonance mismatch due to L_1 on power, but the resonance mismatch due to L_2 deteriorates transmission characteristics, so the capacitor C_2 on the Rx side corrects the resonance mismatch.

3.2. Proposed resonance mismatch compensation method

The residual impedance due to resonance mismatch on the Rx side is denoted as Z_2, which is expressed as follow:

$$Z_2 = \omega_0 L_2 - \frac{1}{\omega_0 C_2} \tag{4}$$

Using Z_2, the Rx side of the LCC-S circuit is shown in Fig. 5.

The current i_1 flowing into the Tx coil is a constant current and the M is constant in static-WPT, so the induced EMF on the Rx side is a constant voltage.

The voltage v_{out_LCCS} on the load is expressed as follows.

$$\left|v_{out\_LCCS}\right| = \left|\frac{\omega_0 M R_L}{R_L + jZ_2} i_1\right| \tag{5}$$

When the resonance mismatch is corrected and $Z_2 = 0$, equation (5) equal to the induced EMF and is independent of the load.

Also at that time, v_{out_LCCS} takes the maximum value. From the above, a load-independent resonance mismatch compensation method is proposed by searching for the maximum value of the v_{out_LCCS} by controlling C_2.

Reference[17] proposes a method for controlling R_L and controlling output power by varying the input impedance of the DC/DC converter. By varying R_L simultaneously with the proposed resonance mismatch correction method, the resonance mismatch can be corrected while keeping the output power constant.

4. Numerical analysis and experimental validation

In this chapter, the theory is verified through numerical analysis and experimental transmission characteristic comparison. The verification is divided into two parts: verification of power robustness against resonance mismatch on the Tx side and verification of the resonance mismatch compensation method for the LCC-S circuit. Experiments were carried out using Keysight's Vector Network Analyzer (VNA) E5061B as shown in Fig. 6 to evaluate the transmission characteristics.

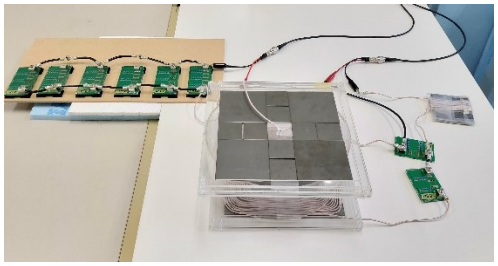

Fig. 6 Overview of the experiment.

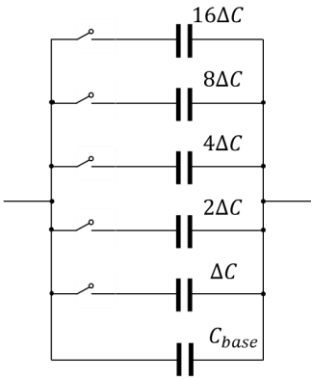

Fig. 7 Overview of variable capacitors

Table 1 PARAMETER

Symbol	Description	Value
f	Operating frequency	85 kHz
E	Input AC Voltage(amp)	20 V
L_0	Tx Compensation inductance	20 μH
C_0	Rx Compensation capacitance	166 nF
L_1	Self-inductance of Tx coil	99 μH
L_2	Self-inductance of Rx coil	97 μH
R_1	Internal resistance of Tx coil	0.3 Ω
R_2	Internal resistance of Rx coil	0.3 Ω
d	Distance between Tx and Rx Coil	10 cm
k	Coupling coefficient	0.208
L_0'	Rx Compensation Inductance	22 μH
C_0'	Rx Compensation Capacitance	167 nF
ΔC	Increment of Capacitance	0.5 nF

4.1. Experimental preparation - how to change capacitance

In this paper, the variable capacitor is created as shown in Fig. 7. At the bottom, a capacitor C_{base} with the minimum value of capacitance is attached. Above it, the total capacitance C_t is varied by attaching $\Delta C, 2\Delta C, 4\Delta C, 8\Delta C$ and $16\Delta C$ in parallel.

The target value is tracked by starting counting from $N = 0$, converting to binary numbers and then turning on the capacitor corresponding to 1. For example, when $N = 1$, only ΔC is switched ON; when $N = 2$, ΔC is switched OFF and $2\Delta C$ is switched ON instead; when $N = 3$, ΔC and $2\Delta C$ are switched ON; when $N = 4$, ΔC and $2\Delta C$ are switched OFF and $4\Delta C$ is switched ON; the search continues until $N = 31$.

When the counter is N, C_t is expressed as follow:

$$C_t = C_{base} + \Delta C \times N \tag{6}$$

By manually changing the capacitance of C_t by changing the capacitor connections, the changes in transmission characteristics were measured.

4.2. Verification of power robustness to resonance mismatch on the Tx side

The color map created by numerical analysis and transmission characteristic evaluation of the LCC-S circuit in Fig. 4 with $R_L = 6\ \Omega$ fixed and varying capacitors C_{1S} and C_{2S} is shown in Fig. 8 and the efficiency color map in Fig.9.

In the experiment, the variable capacitor of Fig. 7 was inserted in C_{1S} on the Tx side, $C_{base} = 39.5$ nF and C_1 was varied from 39.5 ~ 48 nF. The transmission characteristics were obtained by varying the Rx side with VNA.

Fig. 8 (a), (b) shows that, as the theory suggests, resonance mismatch on the Tx side does not affect the change in power, but resonance mismatch on the Rx side does affect the change in power and it is necessary to compensate for the resonance mismatch. Also, Fig. 9 (a), (b) shows that the resonance mismatch on the Tx side has little effect on the efficiency reduction, but the resonance mismatch on the Rx side causes the efficiency reduction. From the above, it was found that the LCC circuit can suppress the effect of resonance mismatch on the Tx side on the power and efficiency. The reason why the efficiency obtained by the experiment in Fig. 9 (b) is not continuous is considered because the ESR is different for each of the capacitors connected in parallel in Fig. 7.

Fig. 8 and Fig. 9 show that no resonance mismatch on the Tx side is required, as both power and efficiency remained unchanged even when C_{1S} deviated from resonance.

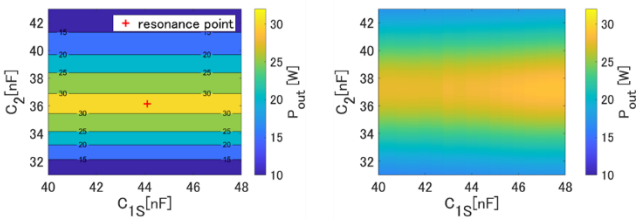

(a) Numerical analysis (b) Experiments

Fig. 8 Relationship between resonance mismatch of Tx and Rx and power (R_L=6 Ω)

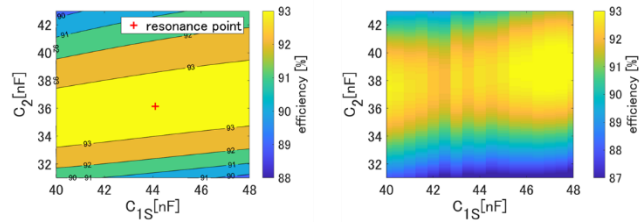

(a) Numerical analysis (b) Experiments

Fig. 9 Relationship between resonance mismatch and efficiency of Tx and Rx. (R_L=6 Ω)

4.3. Verification of a method for correcting resonance mismatch in LCC-S circuits

Numerical analysis and experiments were then carried out on the output power, output voltage and transmission efficiency of the LCC-S circuit when the capacitance C_2 and load R_L were varied, fixed at $C_{1S} = 39.5$ nF in Fig. 4, and a color map was produced. In the experiments, the variable capacitor of Fig. 7 was inserted in C_2 and varied so that $C_2 = 31$~43 nF, with C_{base} placed at 31 nF. R_L was varied by VNA.

The numerical analysis of the output power and the experimental results are shown in Fig. 10 (a), (b) , the numerical analysis of the output voltage and the experimental results in Fig. 11(a), (b) and the numerical analysis of the efficiency and the experimental results in Fig. 12 (a), (b). The red lines in Fig. 10 (a), Fig. 11 (a), Fig. 12 (a) show the capacitors at resonance, respectively. From Fig. 10 (a), (b), at resonance, the output voltage v_{out_LCCS} is maximum irrespective of the value of the load. On the other hand, Fig. 11 (a), (b) shows that the output power varies as the value of the load changes. it is possible to adjust the power due to the load concurrently by searching for the maximum value of the output voltage at C_2. It was also found that high efficiency can be taken as the resonance on the Rx side approaches and the resistance of the load increases. Fig. 12 (a), (b) show different scales of the color map. The lower efficiency in experiment (b) can be attributed to the effect of the ESR of the capacitor.

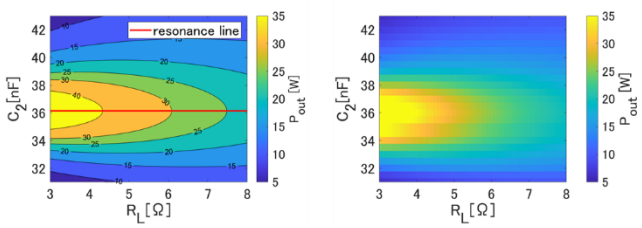

(a) Numerical analysis (b) Experiments

Fig. 10 Relationship between resonance mismatch of Rx side and output power (C_{1S} =39.5 nF)

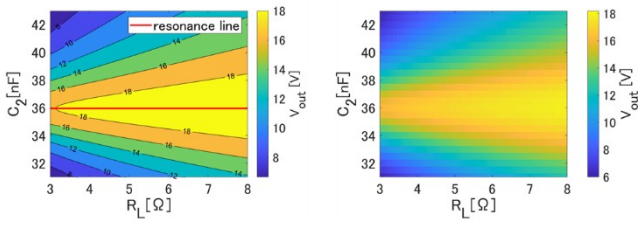

(a) Numerical analysis (b) Experiments

Fig. 11 Relationship between resonance mismatch of Rx side and output voltage. (C_{1S} =39.5 nF)

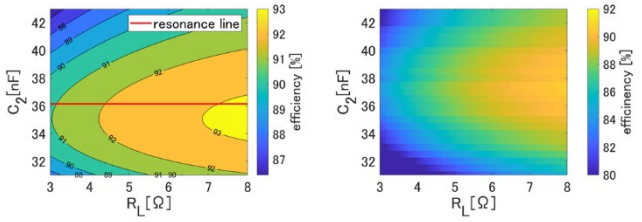

(a) Numerical analysis (b) Experiments

Fig. 12 Relationship between resonance mismatch of Rx side and transmission efficiency. (C_{1S} =39.5 nF)

From the above, it is possible to correct for resonance mismatch in the LCC-S circuit by measuring the output voltage, even if the load is changing.

Also, from Fig. 11, the change in voltage due to the resonance mismatch occurs sharply, especially low values of load resistance. This indicates that the method is suitable for use in regions with low values of load.

5. CONCLUSION

This paper proposes an improvement method to solve the transmission power reduction due to resonance mismatch in wireless power transfer by using the LCC circuit on the Tx side, making the control on the Tx side unnecessary and only controlling the Rx side. The proposed method does not use communication between Tx and Rx and allows the load to fluctuate during the compensation of the resonance. It was found to be possible to compensate for resonance mismatch irrespective of the value of the load.

Future work includes creating a prototype in which the controller of the system is implemented, as well as the implementation of feeding a constant voltage load that simulates a battery instead of a resistive load.

REFERENCES

(1) G. A. Covic and J. T. Boys, “Inductive power transfer,” Proc. IEEE, vol. 101, no. 6, pp. 1276–1289, Jun. 2013.

(2) M. Ruhul Amin and R. B. Roy, "Design and simulation of wireless stationary charging system for hybrid electric vehicle using inductive power pad in parking garage," The 8th International Conference on Software, Knowledge, Information Management and Applications (SKIMA 2014), Dhaka, Bangladesh, 2014, pp. 1-5.

(3) C. G. Colombo, S. M. Miraftabzadeh, A. Saldarini, M. Longo, M. Brenna and W. Yaici, "Literature Review on Wireless Charging Technologies: Future Trend for Electric Vehicle?", 2022 Second International Conference on Sustainable Mobility Applications, Renewables and Technology (SMART), Cassino, Italy, 2022, pp. 1-5.

(4) Y. Lim, H. Tang, S. Lim and J. Park, "An Adaptive Impedance-Matching Network Based on a Novel Capacitor Matrix for Wireless Power Transfer," in IEEE Transactions on Power Electronics, vol. 29, no. 8, pp. 4403-4413, Aug. 2014.

(5) H. Weerasekara, K. Hata, T. Imura and Y. Hori, "Effect of Resonance Frequency Mismatch for Transmission Power in Wireless Power Transfer System," 2019 IEEE Vehicle Power and Propulsion Conference (VPPC), 2019, pp. 1-4

(6) H. Weerasekara, K. Hata, T. Imura, H. Fujimoto and Y. Hori, "Efficiency Maximization in Wireless Power Transfer Systems for Resonance Frequency Mismatch," 2019 IEEE PELS Workshop on Emerging Technologies: Wireless Power Transfer (WoW), 2019, pp. 363-366

(7) SAE International, “Wireless Power Transfer for Light-Duty Plug-in/Electric Vehicles and Alignment Methodology J2954,” Issued2016-05, Revised2020-10.

(8) Y. Lim, H. Tang, S. Lim and J. Park, "An Adaptive Impedance-Matching Network Based on a Novel Capacitor Matrix for Wireless Power Transfer," in IEEE Transactions on Power Electronics, vol. 29, no. 8, pp. 4403-4413, Aug. 2014.

(9) Y. C. Liu, J. Zhang, C. K. Tse, C. Zhu and S. -C. Wong, "General Pathways to Higher Order Compensation Circuits for IPT Converters via Sensitivity Analysis," in IEEE Transactions on Power Electronics, vol. 36, no. 9, pp. 9897-9906, Sept. 2021

(10) Q. Mao, J. Deng, S. Wang and Z. Wang, "A Detuned LCC-LCC Compensation Topology with Coupling Variation Resisting for EV Wireless Charger," 2020 IEEE 9th International Power Electronics and Motion Control Conference (IPEMC2020-ECCE Asia), 2020, pp. 96-100

(11) K. Song et al., "An Impedance Decoupling-Based Tuning Scheme for Wireless Power Transfer System Under Dual-Side Capacitance Drift," in IEEE Transactions on Power Electronics, vol. 36, no. 7, pp. 7526-7536, July 2021

(12) Y. Luo, Y. Yang, S. Zhang, X. Luo and L. Li, "Performance Analysis and Optimization of The MCR-WPT System with Uncertain Parameters," 2020 IEEE Wireless Power Transfer Conference (WPTC), 2020, pp. 154-158

(13) W. Li, Q. Zhang, C. Cui and G. Wei, “A Self-Tuning S/S Compensation WPT System without Parameter Recognition,” in IEEE Transactions on Industrial Electronics.

(14) R. Matsumoto and H. Fujimoto, "Wireless EV Charging System Using PWM-Controlled Variable Capacitor for Maximum Power Transfer under Severe Coil Misalignment," 2022 International Power Electronics Conference (IPEC-Himeji 2022- ECCE Asia), 2022

(15) K. Matsuura, D. Kobuchi, Y. Narusue and H. Morikawa, "Communication-Less Receiver-Side Resonant Frequency Tuning Method for Magnetically Coupled Wireless Power Transfer Systems," 2021 IEEE Radio and Wireless Symposium (RWS), 2021

(16) S. Li, W. Li, J. Deng, T. D. Nguyen and C. C. Mi, "A Double-Sided LCC Compensation Network and Its Tuning Method for Wireless Power Transfer," in IEEE Transactions on Vehicular Technology, vol. 64, no. 6, pp. 2261-2273, June 2015.

(17) K. Lu, Y. Wang, Y. Yao, Y. Guan and D. Xu, "A Novel WPT System with Digitally Closed-loop Control Featuring High Misalignment Tolerance," 2019 IEEE 4th International Future Energy Electronics Conference (IFEEC), Singapore, 2019, pp. 1-6